^{1}H NMR Relaxation Studies of the Micellization of a Poly(ethylene oxide)−Poly(propylene oxide)−Poly(ethylene oxide) Triblock Copolymer in Aqueous Solution

Franco Cau and Serge Lacelle*

Département de Chimie, Université de Sherbrooke, Sherbrooke, Québec, Canada J1K 2R1

Received July 10, 1995; Revised Manuscript Received September 26, 1995[⊗]

ABSTRACT: ^{1}H nuclear magnetic resonance (NMR) relaxation studies of the temperature-induced micellization of a poly(ethylene oxide)−poly(propylene oxide)−poly(ethylene oxide), PEO−PPO−PEO, block copolymer in aqueous solution were performed in the range 280−345 K. ^{1}H NMR spectra of the block copolymer were well resolved, thus allowing us to probe specifically the methyl and methylene relaxation processes in the PPO and PEO blocks, respectively. Interpretation of the relaxation data in terms of the Hall−Helfand correlation function leads to four distinct correlation times for the PPO and PEO blocks. The slower correlation time in the PPO block was identified as the Zimm−Rouse first normal mode of the copolymer and served to determine the hydrodynamic radius, R_H, of the unimers and the micelles. On a more local scale, the behavior of the correlation time for segmental motions in the PPO block indicates an extension of the PPO chains in micelles relative to the unimers. This conformational change is related to the formation of a water insoluble liquid-like core created by the PPO chains in the micelle where the trans isomers are favored. The rotational isomeric states model used to interpret the faster correlation time in the PEO chains yields an activation energy of 14.6 kJ/mol for the correlated transitions in the PEO blocks, in agreement with previous theoretical calculations. The slower correlation time in the PEO blocks shows a marked increase upon micellization attributed in part to the polymer−polymer interactions between the different PEO blocks constituting the hydrophilic moiety of the micelles. A power law relating this relaxation time to the micelle hydrodynamic radius is predicted and observed experimentally. The concentration dependence of the critical micellization temperature, inferred from the methyl spin−lattice relaxation time in the PPO block, was found to be adequately described by a closed association model. The standard free energy, enthalpy, and entropy of micellization obtained by NMR are in close agreement with the recent experimental thermodynamic studies of P. Alexandridis *et al.* (*Macromolecules* **1994**, *27*, 2414).

I. Introduction

Water-soluble triblock copolymers of poly(ethylene oxide) (PEO) and poly(propylene oxide) (PPO) with structure PEO−PPO−PEO are nonionic macromolecular surfactants widely used in industrial technological processes as detergents, emulsifiers, wetting agents, and dispersion stabilizers.[1,2] Due to their amphiphilic nature and low toxicity, they also serve as controlled drug delivery systems[3,4] and protect microorganisms against mechanical damages in bioreactors.[5,6]

The temperature−concentration phase diagram of aqueous PEO−PPO−PEO block copolymer solutions exhibits different structural regions which become more ordered with increasing temperature and concentration.[7] In the dilute regime and at low temperatures, the block copolymers behave as independent chains dissolved in the aqueous solvent. The block copolymer structure has been probed in these solutions through surface tension studies, from which it was inferred that the block copolymer forms a PPO hydrophobic core surrounded by the hydrophilic PEO blocks.[8−10] With increasing temperature, a critical micellization temperature, T_{CMT}, is observed where aggregation of the PEO−PPO−PEO block copolymers occurs and leads to the formation of intermolecular micelles. The T_{CMT} decreases with increasing concentration or the fraction of hydrophobic PPO residues in the block copolymers.[11] Numerous experimental studies (static and dynamic light-scattering, small angle neutron scattering (SANS), pulsed field gradient NMR, viscosity measurements) have shown that in a broad temperature range above T_{CMT}, spherical micelles, formed by a dense hydrophobic core of PPO with a PEO shell, coexist in solution with unimers.[12−15] Furthermore, thermodynamic analysis of the micellization processes suggests that a dynamical equilibrium, N unimers $\rightleftarrows$ micelle, where N is the aggregation number, arises during the micelle formation. This equilibrium can be described by a closed association model with an association−dissociation equilibrium between the N unimers and micelles.[11,16] For this equilibrium, the aggregation number N increases with temperature.[17] Eventually, a second critical temperature is reached where all unimers have aggregated. For some PEO−PPO−PEO block copolymers, a conformational change from spherical to rodlike structure ensues when the core diameter of the micelles becomes comparable to the length of the fully stretched PPO chain of the PEO−PPO−PEO block copolymer.[18] In the concentrated regime, micelle formation is still observed at lower temperatures. In addition, when the volume fraction of the micelles in solution exceeds 0.53, a thermoreversible gel transition, called "inverse melting transition", occurs where the micelles crystallize into a body-centered cubic lattice.[19] At still higher temperatures, and in the whole concentration range, a cloud point is reached and the copolymer solution becomes opaque due to phase separation.

Earlier NMR studies of the PEO−PPO−PEO block copolymers have mainly focused on the assignments of ^{1}H and ^{13}C chemical shifts.[20−22] The temperature dependence of the chemical shifts and the line shape of the ^{13}C resonance of the methyl groups in the PPO block were used to probe the hydrophobic region of the copolymer during the micellization processes. Slight

* To whom correspondence should be addressed.

[⊗] Abstract published in *Advance ACS Abstracts,* December 1, 1995.

0024-9297/96/2229-0170$12.00/0

variations in the line position and broadening of the line width of the methyl resonance were attributed to a dehydration process which induces a conformational change involving alternations in the orientations and steric crowding of the methyl groups.[20] Pulsed field gradient NMR (PFG NMR) techniques, which were used to measure the self-diffusion coefficients of the unimers and the micelles, provided an alternative approach to classical scattering techniques for the determination of the hydrodynamic radii of the PEO−PPO−PEO block copolymer.[12,23] However, as scattering methods, PFG NMR techniques are solely sensitive to large scale motions, i.e., the overall translational motion of the unimers or the micelles in solution, and are less affected by the local dynamics and internal structures of the diffusing species. While extensive NMR relaxation studies of polymers in solution have demonstrated the sensitivity of the spin relaxation processes to fast local motions in polymer chains,[24] it appears that the use of NMR relaxation measurements to investigate micellization processes has been restricted to rather small surfactant systems, where single exponential time-correlation functions are widely used to interpret the NMR data.[25] It is generally concluded from such studies that nuclear spin relaxation is mainly determined by fast segmental motions of the backbone surfactant chains and by the overall rotational tumbling of the surfactant micelles.[26] In order to correctly interpret NMR relaxation data in cases where micelles are formed by long polymer chains, it is necessary to use a more realistic model for the time-correlation function describing segmental motions of the individual polymer chains. In the present ^{1}H NMR relaxation studies of the micellization processes in aqueous PEO−PPO−PEO block copolymer solutions, the relaxation of the methylene protons in the PEO blocks and of the methyl protons in the PPO block were analyzed on the basis of the Hall−Helfand model for the local segmental dynamics of a polymer chain.[27] In this model, chain dynamics are based on local conformational changes (correlated transitions) which propagate along the chain according to a damped diffusional process (single transitions). The shape of the resulting time-correlation function is non-exponential, and the corresponding spectral density function becomes a function of the two time constants characterizing the correlated and the single transitions of the chains. Hence, from the experimental relaxation measurements, it is possible to obtain a local characterization of the segmental dynamics in each part of the block copolymers within the micelles. Furthermore, the structural changes within the PEO−PPO−PEO block copolymer associated with the unimers−micelles transition affect the time constants of the segmental relaxation mechanisms and, thus, alter the observed NMR relaxation times of the protons in each part of the copolymers.

II. Experimental Section

The ^{1}H NMR experiments were performed on a Bruker WM 250 spectrometer operating at 250 MHz. The following conditions were used throughout unless explicitly stated: 6.3 μs 90° radio-frequency pulses, quadrature detection with the CYCLOPS phase cycling scheme, 1.5 kHz spectral width corresponding to 6 ppm, 1.9 kHz filter bandwidth, acquisition of 1024 complex data points per transient every 8 s, accumulation of 4−128 free induction decays (FIDs), and zero-filling of the data to 4096 points before Fourier transformation. The spin−lattice relaxation times T_1 were measured with the inversion-recovery method. For the methyl group, the spin−spin relaxation times T_2 were obtained from the decays of the Carr−Purcell−Meiboom−Gill spin echoes. For the methylene protons of the PEO blocks in the 9% solution, T_2 values were determined from the line width measurements with a correction for inhomogeneous line broadening. A nonlinear least-squares fitting routine from Bruker was used to extract T_1 and T_2 values. The temperature was controlled to ±0.3 deg and calibrated with a copper−constantin thermocouple. At each temperature, a delay of 15 min allowed the stabilization of the sample temperature before the acquisition of the data. Sample rotation was set at 20 ± 1 Hz. Chemical shifts were measured from residual protons in the D_2O solvent, while the D_2O signal served for the lock. Samples of the block copolymer of PPO and PEO, with a structure

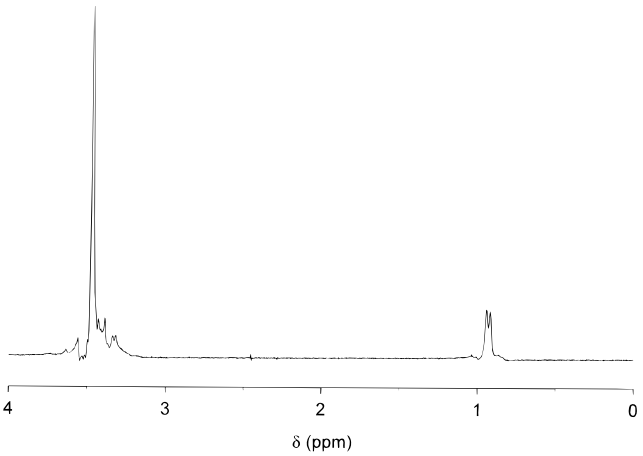

Figure 1. ^{1}H NMR spectrum of the PEO−PPO−PEO block copolymer 1% (w/v) in D_2O at 295 K.

$$HO-[CH_2CH_2O]_n-[CH_2CH(CH_3)O]_m-[CH_2CH_2O]_n-H$$

were obtained from PolyScience Inc. and were generously provided by Professor C. Jolicoeur of the Chemistry Department of the Université de Sherbrooke. In previous studies, the molar mass of the block copolymer of 11 360 g/mol and a PEO/PPO ratio of 1/0.289 had been determined.[28] The molecular weight of the poly(ethylene oxide) sample was 15 000. Samples were dissolved in D_2O (99.9% Merck), and concentrations are reported in % weight/volume extending in a range from 0.02% to 9%.

III. Results

The ^{1}H NMR spectrum of a 1% solution of the PEO−PPO−PEO block copolymer in D_2O at 295 K is presented in Figure 1. Assignments of the chemical shifts of the different resonances attributed in previous studies[22] correspond well to the present measurements. The resonance of the methyl groups of the PPO block is seen as a doublet at 0.9 ppm. The splitting of 7 Hz arises from the J coupling of the methyl protons to the adjacent methyne proton whose resonance is found at 3.35 ppm. The methyne proton being coupled to the methyl and methylene groups in the PPO segment produces a broad resonance. These methylene groups in slightly different chemical environments resonate at 3.54 and 3.68 ppm. The methylene groups of the PEO block produce the intense singlet at 3.48 ppm. The intensities of the resonances of the methylene of the PEO block and the methyl groups of the PPO block serve to measure the relative amount of PEO/PPO. The PEO/PPO ratio determined from the NMR spectral areas is 1/0.289 in agreement with previous studies.[28] This ratio yields an average number of monomer units of $n = 93$ and $m = 54$ in the PEO and PPO blocks, respectively. The presence of well-resolved resonances in the NMR spectra allows us to conveniently monitor the chemical

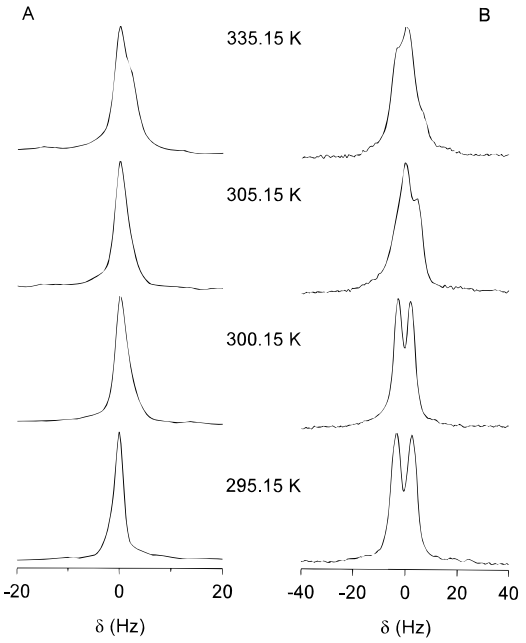

Figure 2. Temperature dependence of the ^{1}H NMR line shapes of the PEO−PPO−PEO block copolymer 1% (w/v) in D_2O: (A) methylene protons in the PEO block; (B) methyl protons in the PPO block.

environment and relaxation at different sites in each block as a function of the temperature. For the practical consideration of signal/noise, the resonances of the methyl of the propylene oxide segment in the PPO block and the methylene of the ethylene oxide segment in the PEO blocks were used as intrinsic probes.

The chemical shifts of both the methyl of PPO and the methylene of PEO in the PEO−PPO−PEO block copolymer showed a linear dependence with the temperature in the range 280−345 K (data not shown). With increasing temperature, the methyl resonance of the PPO block exhibited a downfield shift from 0.82 to 1.25 ppm while the resonance of the methylene in the PEO segments changed from 3.3 to 4.2 ppm. Identical chemical shifts and temperature dependences were also observed for the resonance of the methylene groups in a single chain of PEO (molecular weight 15 000) in D_2O (data not shown). This indicates that the methylene in the PEO segments of the PEO−PPO−PEO block copolymer has a local chemical environment identical to that of the methylene groups in poly(ethylene oxide). These results lend support to the idea that the PEO blocks are in contact with the solvent and segregated from the PPO hydrophobic core.[29] Interestingly, however, the linear variations of the chemical shifts with temperature of both methylene groups of PEO and methyl groups of PPO appeared unaffected in this temperature range where dilatometry studies have inferred micellization of the same PEO−PPO−PEO block copolymer.[28]

The ^{1}H NMR line shapes of the methyl resonance of the PPO block and the methylene resonance of the PEO blocks in the PEO−PPO−PEO block copolymer are displayed in Figure 2 for temperatures ranging from 295 to 335 K, for a 1% (w/v) aqueous solution with $T_{CMT} = 299.15 \pm 1$ K. While the methylene line shape remains relatively constant, the methyl resonance changes considerably. At low temperatures the splitting of the resonance due to the J coupling of the methyl group to the methyne group is resolved. With increasing temperature the line shape broadens and the J splitting

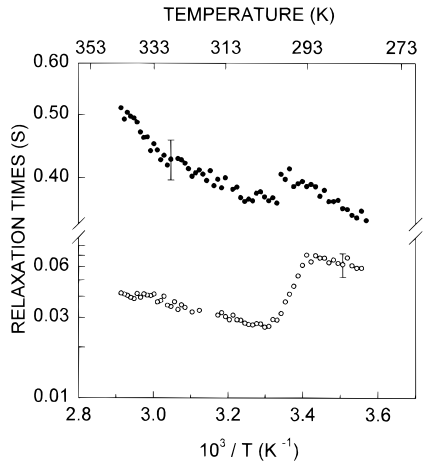

Figure 3. Temperature dependence of the spin−lattice relaxation time T_1 (filled circles) and spin−spin relaxation time T_2 (empty circles) of the methyl protons in the PPO block of the PEO−PPO−PEO block copolymer 9% (w/v) in D_2O. The representative error bars correspond to ± one standard deviation on the relaxation time measurements.

disappears. Above 313 K the shape of the methyl resonance remains constant with a slight reduction in the width up to 343 K. These temperature dependent features of the line shape indicate a change in the chemical environment and/or the orientation of the methyl groups. Averaging of the J coupling by motional processes would lead to a sharp singlet at higher temperatures. A dispersion of local chemical environments, however, would produce a superposition of doublets, resulting in the observed line shape at higher temperatures. These results are consistent with conformational changes occurring in the PPO block. Similar results were also inferred from ^{13}C NMR line shape and chemical shift studies of PEO−PPO−PEO block copolymers.[20] The absence of modifications of the line shape of the methylene in the PEO blocks suggests a constant local chemical environment in the PEO blocks with increasing temperature.

The temperature variation of the spin−lattice relaxation times T_1 and the spin−spin relaxation times T_2 of the PPO methyl protons and the PEO methylene protons are presented in Figure 3 for a 9% w/v PEO−PPO−PEO block copolymer solution. Similar results were obtained for solutions of 0.02, 0.1, 1, 3, 5, and 7% w/v (data not shown). From 293 to ∼303 K the relaxation times of the methyl protons exhibit a sudden decrease (see Figure 3), implying motional changes in the PPO block. This transition temperature in the NMR relaxation behavior coincides with the changes in the partial molar volume and the expansibility observed in dilatometry studies for the same block copolymer in aqueous solution.[28] If one associates the temperature where the relaxation times change abruptly with the critical micellization temperature, T_{CMT}, of the copolymer solution, then the standard free energy of micellization $\Delta G°$ can be calculated from[11]

$$\Delta G° = RT_{CMT} \ln(x) \qquad (1)$$

where R is the gas constant and x is the concentration in mole fraction units, yielding $\Delta G° = -21.6$ kJ/mol from the NMR data of the 9% copolymer solution. This value agrees well with $\Delta G° = -21.1$ kJ/mol obtained from an empirical equation relating $\Delta G°$ to the molecular weight, concentration, and number of monomer units in the

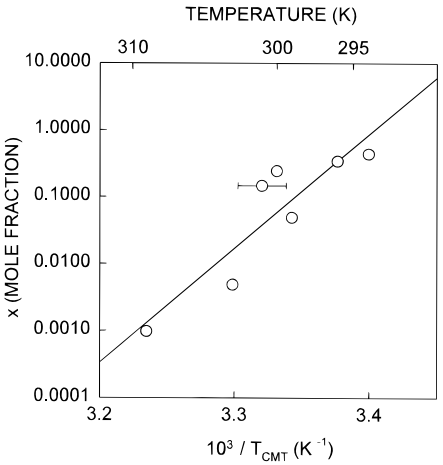

Figure 4. Semilogarithmic plot of the mole fraction x of the PEO−PPO−PEO block copolymer in D_2O versus the inverse of the critical micellization temperature, $1/T_{CMT}$. The line represents the result of the linear least-squares regression on experimental data. The typical error bar corresponds to the maximum uncertainty on the determination of T_{CMT} from NMR relaxation data.

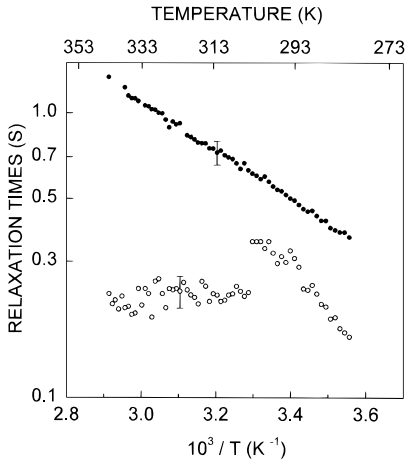

Figure 5. Temperature dependence of the spin−lattice relaxation time T_1 (filled circles) and spin−spin relaxation time T_2 (empty circles) of the methylene protons in the PEO blocks of the PEO−PPO−PEO block copolymer 9% (w/v) in D_2O. The representative error bars correspond to ± one standard deviation on the relaxation time measurements.

PEO−PPO−PEO block copolymer.[11] Moreover, the standard enthalpy of micellization, $\Delta H°$, can be extracted from the concentration dependence of T_{CMT} since[11]

$$\Delta H° = R\left[\frac{\partial \ln(x)}{\partial(1/T_{CMT})}\right]_P \qquad (2)$$

A plot of $\ln(x)$ versus $1/T_{CMT}$ should therefore be linear, with a slope given by $\Delta H°/R$. Such a plot is shown in Figure 4 together with the result of the linear regression. In accordance with eq 2, one obtains $\Delta H° = 374 \pm 75$ kJ/mol or $\Delta H° = 1.6 \pm 0.3$ kJ/(mol of monomer units). The latter value is comparable with the experimental enthalpies of micellization determined on a large number of PEO−PPO−PEO block copolymers of different molecular weights and different polymer composition ratios PPO/PEO.[30] Finally, the standard entropy of micellization, $\Delta S°$, is obtained directly from $\Delta S° = (\Delta H° - \Delta G°)/T_{CMT}$. Numerical evaluation with the NMR data yields $\Delta S° = 1.4 \pm 0.3$ kJ/(mol K) for the 9% copolymer solution, in accord with the data presented in ref 11. Therefore, this thermodynamic analysis shows that the observed transition in the relaxation times of the methyl groups in the PPO block arises from the aggregation of PEO−PPO−PEO block copolymers. The influence of the micellization processes on the spin−spin and spin−lattice relaxation times of the methylene protons of the PEO blocks was also monitored for the 9% solution (see Figure 5). It is somewhat surprising that the PEO T_1 is insensitive to the structural changes which occur during the micellization of the block copolymer. Indeed, over the entire temperature range, T_1 obeys a simple Arrhenius law, i.e., $T_1 = T_0 \exp[E_a/(RT)]$, with an apparent activation energy $E_a = 16.3 \pm 0.1$ kJ/mol, comparable with the apparent activation energies found in dilute poly(ethylene oxide) solutions.[31] While T_2 variations can be similarly described by an Arrhenius law below the critical micellization temperature with an apparent activation energy of 34 ± 2 kJ/mol, this dependence breaks down above T_{CMT} with a subsequent drop to a constant value, $T_2 = 0.23 \pm 0.02$ s.

IV. Interpretation

Quantitative analysis of molecular motions and relaxation in polymer solutions provides relationships between the relaxation rates T_2^{-1}, T_1^{-1}, internuclear distances, the resonance frequency and the frequency spectra of molecular motions. For protons, the principal mechanism of relaxation is through the time dependent dipolar interactions. The autocorrelation function of this interaction is inversely proportional to the inverse sixth power of the distance between the coupled spins; thus, only the dipolar interaction among geminal protons will be considered here. For the same reason, cross relaxation between different proton groups within the polymer can also be neglected. The relaxation rates for protons are given by[32]

$$\frac{1}{T_1} = \frac{6}{20}\gamma^4\hbar^2 r^{-6}[J(\omega_0) + 4J(2\omega_0)] \qquad (3)$$

$$\frac{1}{T_2} = \frac{3}{20}\gamma^4\hbar^2 r^{-6}[3J(0) + 5J(\omega_0) + 2J(2\omega_0)] \qquad (4)$$

where γ is the proton magnetogyric ratio, $\hbar$ is Planck's constant divided by 2π, r is the internuclear distance, and $J(\omega)$ is the spectral density function at different frequencies, ω_0 being the Larmor frequency.

In order to apply this formalism to the PEO−PPO−PEO block copolymer, we will use the spectral density function derived from the Hall−Helfand (HH) time-correlation function for the local dynamics of a polymer chain.[27] For the methylene protons of the PEO blocks $J(\omega)$ is given by[33,34]

$$J(\omega) = A[\{\tau_{sin}^{-1}(\tau_{sin}^{-1} + 2\tau_{cor}^{-1}) - \omega^2\}^2 + \{2(\tau_{sin}^{-1} + \tau_{cor}^{-1})\omega\}^2]^{-1/4} \qquad (5)$$

where τ_{sin} represents the correlation time for single, uncorrelated long-range motions and τ_{cor} is the correlation time for combined, correlated short-range motions. The prefactor $A(\omega)$ takes the form

$$A(\omega) = \cos\left[\frac{1}{2}\arctan\left(\frac{2(\tau_{sin}^{-1} + \tau_{cor}^{-1})\omega}{\tau_{sin}^{-1}(\tau_{sin}^{-1} + 2\tau_{cor}^{-1}) - \omega^2}\right)\right]$$

The HH model combined with anisotropic jumps among three minima separated by 120° yields the following expression for the spectral density function, $J_r(\omega)$, of the internal rotation of a methyl group[35]

$$J_r(\omega) = A_r J_a(\tau_{sin},\tau_{cor},\omega) + B_r J_b(\tau_c,\tau_{cor},\omega) \qquad (6)$$

where

$$A_r = \frac{1}{4}(3\cos^2\Delta - 1)^2 \qquad B_r = \frac{3}{4}(\sin^2 2\Delta + \sin^4\Delta)$$

and

$$\tau_c^{-1} = \tau_{cor}^{-1} + \tau_{rot}^{-1}$$

In these expressions, Δ is the angle between the internuclear vector joining two methyl protons and the axis of rotation of the methyl group and τ_{rot} is the correlation time for the methyl internal rotation. The forms of J_a and J_b are identical as in eq 5 with τ_{sin} replaced by τ_{sin} and τ_c, respectively. It should be pointed out that the present ^{1}H NMR relaxation studies determine the two characteristic times of the HH correlation function from the independent spin−spin and spin−lattice relaxation time measurements at one Larmor frequency, as suggested recently.[34] This procedure is equivalent to previous NMR investigations which have evaluated the correlation times of the HH model solely on the basis of independent spin−lattice relaxation measurements performed at two or more different Larmor frequencies.[33,35,36]

For the geminal protons of the methylene groups in the PEO blocks, the two correlation times characterizing the segmental dynamics can be obtained directly from experimental T_1 and T_2 measurements. Indeed, substitution of eq 5 in eqs 3 and 4 leads to two equations with two unknowns which can be solved for τ_{sin}(PEO) and τ_{cor}(PEO). However, in the case of the methyl relaxation in the PPO block, we have two equations with three unknowns, τ_{sin}, τ_{cor}, and τ_{rot}. As shown by previous NMR relaxation studies on PPO, rapid rotation of the methyl group is an intramolecular process, independent of the local environment,[37] with the same correlation times in the melt as in dilute solutions.[38] A similar behavior for the methyl groups in closed-packed protein molecules was also observed by neutron diffraction.[39] In addition, fast rotation reduces the geminal proton−proton dipolar interaction by a factor $(3\cos^2\Delta - 1)^2/4$ but makes little or no contribution to the relaxation processes.[40] Thus, to a good approximation τ_{rot} is assumed to be solely a function of the temperature through an Arrhenius law, i.e.,

$$\tau_{rot} = \tau_{rot,\infty} \exp\left(\frac{E_a}{RT}\right) \qquad (7)$$

where E_a is the activation energy for the CH_3 group reorientation and $\tau_{rot,\infty}$ is the correlation time at infinite temperature. In order to obtain the most reliable estimate of E_a and $\tau_{rot,\infty}$ in eq 7, a compilation of experimental NMR data for τ_{rot} in PPO is summarized in an Arrhenius plot (see Figure 6). A linear least-squares fit yields $E_a = 13.6 \pm 0.5$ kJ/mol and $\tau_{rot,\infty} = (7 \pm 3) \times 10^{-14}$ s. The results agree with the activation energy obtained by inelastic light scattering, $E_a = 13.8$ kJ/mol,[41] and with the infinite temperature limit value, $\tau_{rot,\infty} = 6.4 \times 10^{-14}$ s, as calculated by Stejskal and Gutowsky.[42] Using the above parameters, it is therefore possible to estimate τ_{rot} at each temperature. Substitution of eqs 5 and 6 in eqs 3 and 4 yields again a set of two equations with two unknowns, τ_{sin}(PPO) and τ_{cor}(PPO). Therefore, at each temperature of the aqueous PEO−PPO−PEO block copolymer solution, the determination of T_1 and T_2 of the methylene protons in the PEO blocks and of the methyl protons in the PPO block, for which an internal reorientation governed by an Arrhenius law is assumed, allows us to determine two distinct correlation times characterizing single and correlated segmental motions in each block of the copolymer. In order to extract motional correlation times, numerical resolution of the resulting two sets of equations were performed with the Newton method implanted in the software Mathematica version 2.2.3 from Wolfram Research. The four resulting correlation times obtained at different temperatures by this method are displayed in Figure 7. Discussion of the behavior of these correlation times follows in succession: τ_{sin}(PPO), τ_{cor}(PPO), τ_{cor}(PEO), and τ_{sin}(PEO).

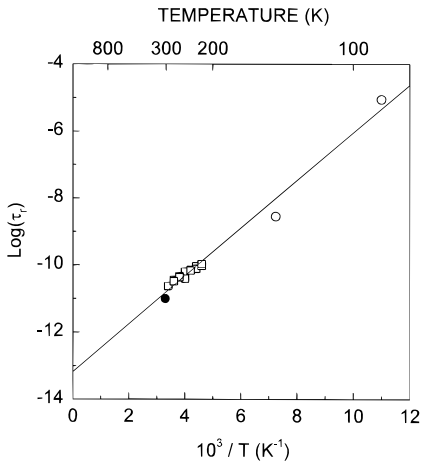

Figure 6. Arrhenius plot of the methyl correlation time, τ_{rot}, in PPO: empty circles, ref 67; empty squares, ref 37; filled circle, ref 38.

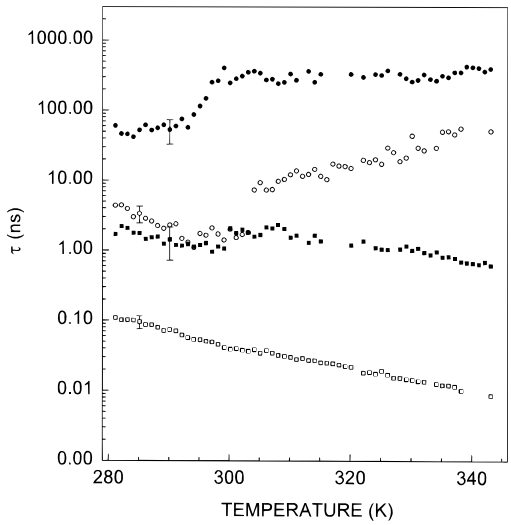

Figure 7. Temperature variation of the correlation times obtained from T_1 and T_2 measurements, using the Hall−Helfand correlation function. Filled and empty symbols correspond to the protons of the methyl groups in the PPO blocks and methylene protons in the PEO blocks, respectively. Circles and squares represent the correlation times for single and correlated motions, respectively. The representative error bars correspond to the deviation on the correlation time calculation arising from ± one standard deviation on the NMR relaxation time measurements.

Below the critical micellization temperature, where only unimers coexist in solution, slow motions in the PPO block are characterized by a constant relaxation time, $\tau_{sin}(PPO) = 55 \pm 30$ ns in the temperature range 281 K < T < 293 K. It is noteworthy to compare the experimental value of $\tau_{sin}(PPO)$, which is the slower correlation time in the unimer (see Figure 7), with the longest internal relaxation time estimated according to the Rouse−Zimm model:[43]

$$\tau_n = \frac{M\eta_0[\eta]}{0.293RT\lambda_n} \tag{8}$$

where M is the molar mass of the polymer, η_0 is the solvent dynamical viscosity, $[\eta]$ is the intrinsic viscosity, R is the gas constant, and T is the temperature. λ_n are given in ref 44; for the longest internal relaxation time, τ_1, $\lambda_1 = 4.04$. Magnetic resonance correlation times are normally concerned with the second-order spherical harmonics contributions in the position coordinates and it can be shown that $\tau_{NMR} = \tau_n/3$.[45] For a PEO chain of molar weight 11 360 with $[\eta]$ = 20 mL/g for PEO in water[46] and η_0 = 1.248 mPa·s for D_2O at 293 K,[47] numerical evaluation of eq 8 yields $\tau_1/3 = 33$ ns, which suggests strongly the identification of $\tau_{sin}(PPO)$ with the first Rouse−Zimm mode. This is also supported by the temperature dependence of $\tau_{sin}(PPO)$ (see Figure 7), since the sharp increase of $\tau_{sin}(PPO)$ above $T_{CMT} = 294$ K can be related to the simultaneous increase of the intrinsic viscosity and the effective molar weight appearing in eq 8, as intermolecular aggregation of the block copolymers occurs.[48] However, to the best of our knowledge there does not exist a theoretical explanation for the equivalence between the HH correlation time for single transitions and the correlation time of the first normal mode in the Rouse−Zimm theory of polymers, as suggested by the above arguments. Nevertheless, as demonstrated below, all the quantities (including the size of the unimers and the micelles and the aggregation numbers) calculated with the above assumption are consistent and in quantitative agreement with previous experimental observations on similar triblock copolymers.

In the Rouse−Zimm normal mode theory, the correlation time τ_1 of an ideal polymer chain (Θ condition) at infinite dilution is related to the end to end distance of the chain, R_0, by[49]

$$\tau_1 = \frac{0.398\eta_0 {R_0}^3}{k_B T} \tag{9}$$

where k_B is Boltzmann's constant. At finite concentration c (w/v) of the polymer, the correlation time at finite dilution, τ'_1, is related to τ_1 by the relation[40]

$$\tau'_1 = \tau_1 \exp(k_H[\eta]c) \tag{10}$$

where k_H is the Huggins constant. Assuming that $\tau_{sin}(PPO)$ corresponds to the relaxation time of the first internal normal mode in the PEO−PPO−PEO block copolymer, the end to end distance R_0 is then given by

$$R_0 = \exp\left(-\frac{k_H[\eta]c}{3}\right)\left(\frac{k_B T}{0.133\eta_0}\tau_{sin}(PPO)\right)^{1/3} \tag{11}$$

Note that the temperature variation of the finite concentration correction term in eq 11 is negligible when computing the copolymer hydrodynamic radius at different temperatures, since viscosity measurements in the temperature range 280 K < T < 323 K show that this prefactor varies by less than 17% with a mean value $\langle \exp(-k_H[\eta]c/3)\rangle = 0.6 \pm 0.1$.[50] Numerical estimation of eq 11 at 293 K with η_0 = 1.248 mPa·s[47] and $\tau_{sin}(PPO) = 55 \pm 30$ ns yields $R_0 = 6 \pm 1$ nm. This result can be compared with the end to end distance calculated from

$$R_0 = (C_\infty n l^2)^{1/2} \tag{12}$$

where C_∞ is the so-called characteristic ratio, which is a measure of the effect of short-range interactions within a chain, n is the number of bonds, and l is the average C−C bond length of 0.146 nm in PEO and PPO.[46] For PEO in water, $C_\infty(PEO) \cong 5$.[51] Experimental values of $C_\infty(PPO)$ for PPO in water are not available since PPO is not water soluble. However, in various polar solvents $C_\infty(PPO) \cong C_\infty(PEO)$.[46] With n = 240, numerical evaluation of eq 12 yields $R_0 \cong 5$ nm in accordance with the NMR result. The hydrodynamic polymer radius, R_H, can be obtained from the Einstein relation, which relates the intrinsic viscosity to the copolymer volume fraction in solution, namely,

$$R_H = \left(\frac{3M[\eta]}{10\pi N_a}\right)^{1/3} \tag{13}$$

where M is the molar mass of the copolymer and N_a is Avogadro's number. With $[\eta]$ = 20.1 mL/g at 293.15 K[50] and M = 11 360, eq 13 gives R_H = 3.3 nm. With the above values of R_0 and R_H it is possible to estimate the ratio $\rho = R_G/R_H = R_0/(6^{1/2}R_H)$, where R_G is the polymer gyration radius.[49] For the unimers at 293 K we find ρ = 0.74. This value is close to ρ = 0.778 valid for a homogeneous polymer sphere.[18] On the other hand, flexible polymers in good or Θ solvents have ρ > 1.[52] Similar small values of ρ < 1 were already observed in PEO−PPO−PEO block copolymers.[15] Assuming a spherical polymer model, the NMR result yields R_H = 3.3 ± 0.6 nm for the unimer hydrodynamic radius. Previous studies performed on Pluronics F88 (M = 10 800 g/mol, n = 97, m = 39) and Pluronics 127 (M = 12 500, n = 99, m = 65) measured a unimer hydrodynamic radius of R_H = 2.9 nm and R_H = 3.5 nm, respectively.[53,54] The value of R_H obtained for our block copolymer of molar weight M = 11 360 (n = 93, m = 54) falls within these two limits. Although eq 9 was derived for the Θ condition, which is probably the case for neither the hydrophilic PEO blocks nor the hydrophobic PPO block in an aqueous solution, this assumption is a good approximation for the description of the PEO−PPO−PEO block copolymer in aqueous solution. In order to compute R_H at all temperatures using eq 11, the temperature dependence of the solvent viscosity was determined by the Arrhenius plot $\ln(\eta/T)$ versus $1/T$, in the range 278 K < T < 343 K using the data compiled in ref 47 for deuterium oxide. The temperature dependence of R_H is presented in Figure 8. The same figure shows the micellar aggregation number, N_{AG}, calculated with the relation

$$N_{AG} = \frac{10\pi {R_H}^3 N_a}{3[\eta]M} \tag{14}$$

The micelle hydrodynamic radius ranges between ∼7 nm at low temperatures above the critical micellization temperature to ∼10 nm at higher temperatures. These values are comparable with previous findings on similar

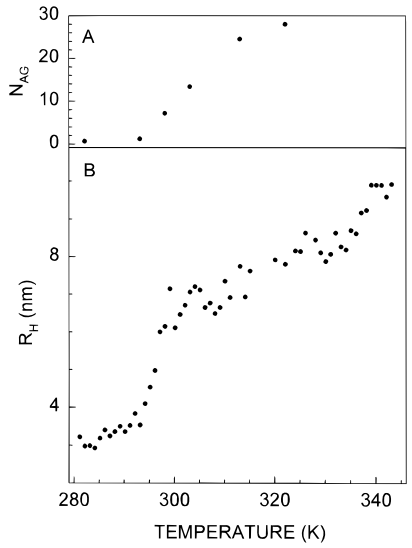

Figure 8. (A) Aggregation number of the PEO−PPO−PEO block copolymer 9% (w/v) versus temperature obtained from NMR measurements and eq 14. (B) Temperature dependence of the effective hydrodynamic copolymer radius in a 9% (w/v) aqueous solution obtained from NMR measurements and eq 13.

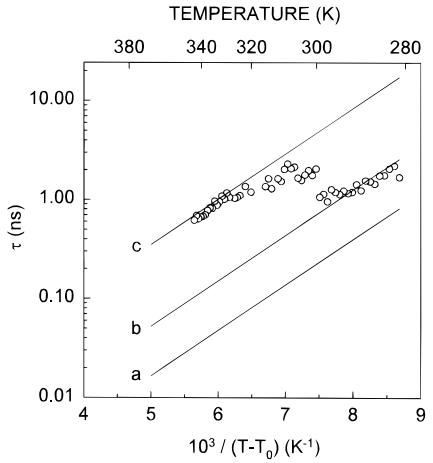

Figure 9. Temperature dependence of the correlation times for segmental motions in PPO chains: (a) segmental mode in melt PPO using the Vogel−Fulcher (VF) model, eq 15, with the coefficients given in ref 59 and with $\tau_0 = 8.4 \pm 10^{-14}$ s; (b) same as (a) with $\tau_0 = 8 \times 10^{-13}$ s; (c) same as (a) with $\tau_0 = 5.3 \times 10^{-12}$ s. Empty circles refer to PPO in the PEO−PPO−PEO block copolymers (present work).

block copolymers, i.e., Pluronics F88 and Pluronics F127.[13,17,53] Note that the micellar aggregation numbers determined in this study agree remarkably well with the theoretical results of Linse[55] and with previous light-scattering studies for the micellization behavior of Pluronics F127.[48] The temperature dependence of N_{AG} is also in qualitative agreement with the SANS studies of Mortensen *et al.* on Pluronics F88 and P85.[7,13]

The correlation time sensitive to the short-range cooperative motions in the PPO chains, τ_{cor}(PPO), remains around ~1 ns in the whole temperature range (see Figure 7). Relaxation times for backbone motions in PPO were also found in the same range.[56] Within experimental errors the same activation energies are obtained for τ_{cor}(PPO) below and above T_{CMT}; $E_s = 26 \pm 3$ kJ/mol and $E_s = 28 \pm 1$ kJ/mol in the unimers and micelles, respectively. These values are close to the activation energies found in bulk PPO for segmental motions. Indeed, NMR measurements give $E_s = 27$,[38] 28.5,[57] and 23 kJ/mol,[58] while the reported value from Rayleigh scattering gives $E_s = 25$ kJ/mol.[56] The activation energy of η/T for the solvent D_2O obtained from ref 47 is 19.5 ± 0.2 kJ/mol. These comparisons clearly suggest that the chain motions of the PPO blocks in micelles and unimers belong to the same transition phenomena as bulk PPO.

In Figure 9, the temperature dependence of τ_{cor}(PPO) is compared with the predictions of the Vogel−Fucher (VF) equation for the segmental (α) mode:[59]

$$\tau_{cor} = \tau_0 \exp\left(-\frac{A}{T - T_0}\right) \qquad (15)$$

where τ_0 and A are constants and T_0 is the Vogel temperature. For PPO, the VF coefficients have been determined by dielectric measurements.[59] In our notation $T_0 = 166$ K, $A = 1057$ K, and $\tau_0 = 8.4 \times 10^{-14}$ s. Note that the loss peak frequency in dielectric measurements is $f = 1/(2\pi\tau_D)$, with the correlation time $\tau_D = 3\tau_{NMR}$. Apart from differences in the prefactor, the agreement between the VF model and nuclear spin relaxation behavior is quite good, indicating that the motional modes described by τ_{cor}(PPO) behave similarly to processes involved in the glass transition phenomenon, as concluded previously in melt PPO.[60] Thus, it may be argued that the PPO blocks in the unimers and micelles form a liquid-like core where the local cooperative segmental motions of the chains are governed solely by the PPO chain properties. Moreover, the significant increase of the correlation time τ_{cor}(PPO) by approximately a factor of 6 at T_{CMT} indicates a more extended conformation of the PPO chains in the micelles. This behavior originates from the conformational change induced by the dehydration of the PEO−PPO−PEO block copolymers during aggregation.[17] Indeed, while the gauche conformers of the O−C−C−O dihedral angles are favored in polar environments and are stabilized by intermolecular hydrogen bondings, the population of trans conformers dominates in nonpolar solvents and in the melt.[61,62] This scenario, combined with the previous observations that unimers are already in an intramolecular micelle-type structure, suggests that unimers are formed by a water impermeable core of the PPO block, with possible hydrogen bondings at the surface, and surrounded by the fully dissolved PEO chains. Similar conclusions were inferred from intrinsic viscosity measurements of oligomeric propylene glycols in water where a hydration factor ranging from 1 to 1.5 water molecules per propylene oxide was found.[63] Thus, the NMR results indicate the presence of a liquid-like core of water-insoluble PPO blocks in both the unimers and micelles. The micellization processes result in a more extended trans conformation of the PPO chains, while hydrogen bonding at the core surface of the unimers stabilizes the less extended gauche conformations.

The correlation times deduced from the T_1 and T_2 measurements of the methylene protons in the PEO blocks are also displayed in Figure 7. The correlation time for short-range combined segmental motions, τ_{cor}(PEO), is found between 0.1 and 0.01 ns in the entire temperature range and is unaffected by the micellization processes of the triblock copolymers. This fast correlation time can be related to the local conformation changes in the flexible PEO chains. Indeed, the time scale of τ_{cor}(PEO) determined in this study is the same as observed for the rotational isomeric transitions in dilute PEO solutions.[64,65] Within the framework of the

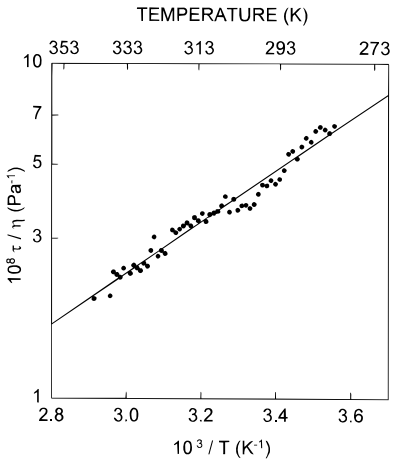

Figure 10. Temperature variation of the faster correlation time in the PEO blocks divided by the solvent viscosity. The line represents the result of the linear least-squares regression on the experimental data points.

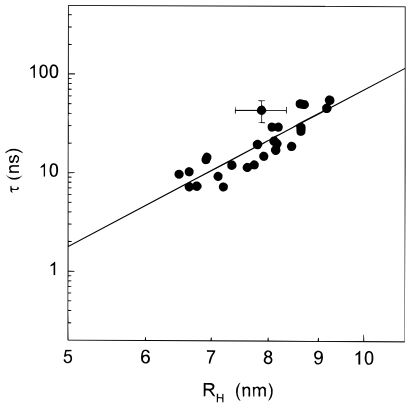

Figure 11. Rotational correlation time for single transitions in the PEO chains of the PEO−PPO−PEO block copolymers, τ_{sin}(PEO), versus the micelle hydrodynamic radius on doubly logarithmic scales. The line represents the result of the linear least-squares regression on the experimental data points. The typical error bars correspond to the maximum uncertainty on the determination of the NMR data.

dynamical rotational isomeric states (RIS) model for local chain dynamics, the correlation time τ for cooperative motions of a few monomer units in the high viscous damping limit can be written as[66]

$$\tau = A\eta_s \exp\left(\frac{E^*}{RT}\right) \tag{16}$$

where A is a constant depending on the shape of the energy minima of the isomeric states, E^* is the activation energy or energy barrier between isomeric minima, and η_s is the solvent dynamical viscosity. Since the solvent viscosity is temperature dependent, the activation energy E^* is obtained from the slope of the Arrhenius plot $\ln(\tau/\eta_s)$ versus $1/T$ (see Figure 10). This procedure yields an activation energy $E^* = 14.6 \pm 0.4$ kJ/mol, comparable to the calculated barrier heights for various conformational transitions in PEO, which range between 9.6 and 15.5 kJ/mol.[66] The above result clearly indicates that local segmental motions in the PEO blocks of the PEO−PPO−PEO block copolymer are unaffected by the micellization processes and proceed as in dilute PEO solutions. In the PEO chains it appears that on a microscopic scale the dynamics of rotational transitions are governed by the solvent viscosity and by conformational jumps.

Unlike the correlation time τ_{cor}(PEO) for cooperative transitions, the slow correlation time for single transitions in the PEO blocks, τ_{sin}(PEO), exhibits a crossover at T_{CMT} (see Figure 7). Below the critical micellization temperature, τ_{sin}(PEO) follows an Arrhenius-type behavior with a rather high activation energy of 63 ± 6 kJ/mol. Although this value is difficult to rationalize at first sight, it should be noted that τ_{sin}(PEO) is of the same order of magnitude as the correlation time for the isotropic rotation of a Kuhn segment, as deduced from NMR relaxation studies of PEO in aqueous solution.[64] Thus, the constant decreasing mobility of the Kuhn subunit above T_{CMT} could be attributed to a progressive entanglement of the PEO chains forming the hydrophilic shell around the PPO core, as the aggregation number increases. A large difference between T_1 and T_2 for the methylene protons of PEO aqueous solutions occurs when polymer−polymer interactions become important.[64] This is precisely what is observed above T_{CMT} (see Figure 5) where T_1 increases while T_2 remains constant. In this case, it is possible to relate the increase of τ_{sin}(PEO) during aggregation to the hydrodynamic radii of the micelles as follows: First, note that the power law $\tau \sim c^2$, where c is the polymer concentration and τ is the rotational correlation time of a spherical domain, holds in semidilute polymer solutions.[49] Moreover, it is expected that $c \sim N_{AG}$, since the number of PEO chains in the shell of the micelles is directly proportional to the aggregation number. Finally, to a good approximation $N_{AG} \sim R_H^3$.[55] Therefore, this dimensional analysis leads to the scaling relation, $\tau \sim R_H^6$, between the rotational correlation time of a Kuhn segment in the PEO chains of the shell and the micelle hydrodynamic radius. The slope of $\log[\tau_{sin}(PEO)]$ versus $\log[R_H]$ in the temperature range 305−345 K gives 5.3 ± 0.6 (see Figure 11) and confirms therefore the predicted dependence of τ_{sin}(PEO) upon the micelle radius of the PEO−PPO−PEO block copolymers.

V. Conclusion

The ^{1}H NMR relaxation studies on the temperature-induced micellization behavior of an aqueous PEO−PPO−PEO block copolymer solution have shown that the local dynamics in each block of the copolymer can be satisfactorily represented by the segmental motions of the backbone chains characterized by the two correlation times of the Hall−Helfand model. The correlation time for isolated, single transitions in the PPO block corresponds to the first normal mode of the Rouse−Zimm theory related to the hydrodynamic radii of the unimers and the micelles of the block copolymers. Quantitative agreement is observed between the copolymers hydrodynamic radii computed from the NMR data and previous light-scattering studies on similar block copolymers. The nature of the cooperative motions of the PPO backbone chains in the PEO−PPO−PEO block copolymer is found to be similar to a glass transition phenomenon in the unimers and in the micelles. The larger time constant of the segmental motions of the PPO chains in the micelles suggests a preferentially more extended, less polar, trans conformation of the PPO chains in the liquid-like core of the micelles, as compared to the more polar, gauche conformation found at low temperatures in the unimer region. Finally, the segmental modes in the PEO blocks are successfully interpreted in terms of the rotational isomeric states model for the correlated conformational transitions, and by considering the rotational correlation

time characterizing the overall tumbling of a Kuhn segment in the PEO chains. The latter exhibits a power law dependence upon the micelle radius, which is predicted by considering the relationships between the concentration of PEO chains in the shell of the micelles, the aggregation number, and the hydrodynamic radius of the micelles.

Acknowledgment. This work was supported by grants from the Natural Sciences and Engineering Research Council of Canada and the FCAR program of the Ministère de l'Education du Québec. Suggestions and discussions with Professor C. Jolicoeur, M. A. Simard, and Dr. F. Quirion are gratefully acknowledged. We would also like to thank S. Bérubé, E. Rouillard, and L. Tremblay for their help at various stages of this work.

References and Notes

(1) Schmolka, I. R. *J. Am. Oil Chem. Soc.* **1977**, *54*, 110.
(2) Lundsted, L. G.; Schmolka, I. R. In *Block and Graft Copolymerization*; Ceresa, R. J., Ed.; Wiley: New York, 1976; Vol. 2.
(3) Park, T. G.; Cohen, S.; Langer, R. *Macromolecules* **1992**, *25*, 116.
(4) Lukowski, G.; Muller, R. H.; Muller, B. W.; Dittgen, M. *Colloid Polym. Sci.* **1993**, *271*, 100.
(5) Jordan, M.; Sucker, H.; Einsele, A.; Widmer, F.; Eppenberger, H. M. *Biotechnol. Bioeng.* **1994**, *43*, 446.
(6) Hua, J.; Erickson, L. E.; Yiin, T.; Glasgow, L. A. *Crit. Rev. Biotechnol.* **1993**, *13*, 305.
(7) Mortensen, K.; Pedersen, J. S. *Macromolecules* **1993**, *26*, 805.
(8) Prasad, K. N.; Luong, T. T.; Florence, A. T.; Paris, J.; Vaution, C.; Seiller, M.; Puisieux, F. *J. Colloid Interface Sci.* **1979**, *69*, 225.
(9) Al-Saden, A. A.; Whateley, T. L.; Florence, A. T. *J. Colloid Interface Sci.* **1982**, *90*, 303.
(10) McDonald, C.; Wong, C. K. *Aust. J. Pharm.* **1977**, *6*, 85.
(11) Alexandridis, P.; Holzwarth, J. F.; Hatton, T. A. *Macromolecules* **1994**, *27*, 2414.
(12) Fleischer, G. *J. Phys. Chem.* **1993**, *97*, 517.
(13) Mortensen, K.; Brown, W. *Macromolecules* **1993**, *26*, 4128.
(14) Mortensen, K. *Prog. Colloid Polym. Sci.* **1993**, *91*, 69.
(15) Wanka, G.; Hoffmann, H.; Ulbricht, W. *Colloid Polym. Sci.* **1990**, *268*, 101.
(16) Kausalya, N.; Fordham, P. J.; Attwood, D.; Booth, C. *J. Chem. Soc., Faraday Trans.* **1990**, *86*, 1569.
(17) Attwood, D.; Collett, J. H.; Tait, C. J. *Int. J. Pharm.* **1985**, *26*, 25.
(18) Schillén, K.; Brown, W.; Johnsen, R. M. *Macromolecules* **1994**, *27*, 4825.
(19) Mortensen, K.; Brown, W.; Nordén, B. *Phys. Rev. Lett.* **1992**, *68*, 2340.
(20) Rassing, J.; McKenna, W. P.; Bandyopadhyay, S.; Eyring, E. M. *J. Mol. Liq.* **1984**, *27*, 165.
(21) Whipple, E. B.; Green, P. J. *Macromolecules* **1973**, *6*, 38.
(22) Ludwig, F. J. *Anal. Chem.* **1968**, *40*, 1620.
(23) Fleischer, G.; Bloss, P.; Hergeth, W-D. *Colloid Polym. Sci.* **1993**, *271*, 217.
(24) Bovey, F. A.; Jelinski, L. W. *J. Phys. Chem.* **1985**, *89*, 571.
(25) Anikin, G. V.; Tomin, O. P. *Colloid J. USSR* **1990**, *52*, 189.
(26) Söderman, O.; Walderhaug, H.; Henriksson, U.; Stilbs, P. *J. Phys. Chem.* **1985**, *89*, 3693.
(27) Hall, C.; Helfand, E. *J. Chem. Phys.* **1982**, *77*, 3275.
(28) Williams, R. K.; Simard, M-A.; Jolicoeur, C. *J. Phys. Chem.* **1985**, *89*, 178.
(29) Zhou, Z.; Chu, B. *Macromolecules* **1987**, *20*, 3091.
(30) In Figure 8 of ref 11, $\Delta H°$ [kJ/(mol of monomer units)] is plotted against the copolymer composition ratio PPO/PEO. In our triblock copolymer, PPO/PEO = 0.289 and the corresponding enthalpy of micellization $\Delta H° = 1.6 \pm 0.3$ kJ/(mol of monomer units) yields a point within the experimental data points and close to the best fit presented in Figure 8 of ref 11.
(31) Liu, K. J.; Ullman, R. *J. Chem. Phys.* **1968**, *48*, 1158 and references therein.
(32) Solomon, I. *Phys. Rev.* **1955**, *99*, 559.
(33) Connolly, J. J.; Jones, A. A. *Macromolecules* **1985**, *18*, 906.
(34) Sinha, B. R.; Blum, F. D.; Schwab, F. C. *Macromolecules* **1993**, *26*, 7053.
(35) Ratto, J. A.; Inglefield, P. T.; Rutowski, R. A.; Li, K-L.; Jones, A. A.; Roy, A. K. *J. Polym. Sci., Polym. Phys. Ed.* **1987**, *25*, 1419.
(36) Dejean de la Batie, R.; Lauprêtre, F.; Monnerie, L. *Macromolecules* **1989**, *22*, 2617.
(37) Heatley, F.; Begum, A. *Polymer* **1976**, *17*, 399.
(38) Heatley, F. *Polymer* **1975**, *16*, 493.
(39) Kossiakoff, A. A.; Shteyn, S. *Nature* **1984**, *311*, 582.
(40) Jones, A. A.; Lubianez, R. P. *Macromolecules* **1978**, *11*, 126.
(41) Higgins, J. S.; Allen, G.; Brier, P. N. *Polymer* **1972**, *13*, 157.
(42) Stejskal, E. O.; Gutowsky, H. S. *J. Chem. Phys.* **1958**, *28*, 388.
(43) Zimm, B. H. *J. Chem. Phys.* **1956**, *24*, 269.
(44) Zimm, B. H.; Roe, G. M.; Epstein, L. F. *J. Chem. Phys.* **1956**, *24*, 279.
(45) Bullock, A. T.; Cameron, G. G. In *Structural Studies of Macromolecules by Spectroscopic Methods*; Ivin, K., Ed.; J. Wiley & Sons: London, 1976; Chapter 15.
(46) *Polymer Handbook*; Brandrup, J., Immergut, E. H., Eds.; J. Wiley & Sons: New York, 1989.
(47) Hydrocarbons. *TRC Thermodynamic Tables*; Thermodynamics Research Center, Texas A&M University: College Station, TX, 1985; Vol. 2, pp C-30−32.
(48) Rassing, J.; Attwood, D. *Int. J. Pharm.* **1983**, *13*, 47.
(49) Doi, M.; Edwards, S. F. *The Theory of Polymer Dynamics*; Oxford University Press: New York, 1986.
(50) Quirion, F. Unpublished results.
(51) Chew, B.; Couper J. *J. Chem. Soc., Faraday Trans. 1* **1973**, *72*, 382.
(52) Douglas, J. F.; Freed, K. F. *Macromolecules* **1984**, *17*, 2354.
(53) Brown, W.; Schillén, K.; Hvidt, S. *J. Phys. Chem.* **1992**, *96*, 6038.
(54) Malmsten, M.; Lindman, B. *Macromolecules* **1992**, *25*, 5440.
(55) Linse, P. *Macromolecules* **1993**, *26*, 4437.
(56) Jones, D. R.; Wang, C. H. *J. Chem. Phys.* **1976**, *65*, 1835.
(57) Connor, T. M.; Blears, D. J.; Allen, G. *Trans. Faraday Soc.* **1965**, *61*, 1097.
(58) Manning, J. P.; Frech, C. B.; Fung, B. M.; Frech, R. E. *Polymer* **1991**, *32*, 2939.
(59) Schlosser, E.; Schönhals, A. *Prog. Colloid Polym. Sci.* **1993**, *91*, 158 and references therein.
(60) Dejean de la Batie, R.; Lauprêtre, F.; Monnerie, L. *Macromolecules* **1988**, *21*, 2052.
(61) Björling, M.; Karlström, G.; Linse, P. *J. Phys. Chem.* **1991**, *95*, 6706.
(62) Williams, G. *Trans. Faraday Soc.* **1965**, *1*, 1564.
(63) Sandell, L. S.; Goring, D. A. I. *Macromolecules* **1970**, *3*, 50.
(64) Breen, J.; Van Duijn, D.; De Bleijser, J.; Leyte, J. C. *Ber. Bunsen-Ges. Phys. Chem.* **1986**, *90*, 1112.
(65) Lang, M-C.; Lauprêtre, F.; Noël, C.; Monnerie, L. *J. Chem. Soc., Faraday Trans. 2* **1979**, 75.
(66) Bahar, I.; Erman, B.; Monnerie, L. *Macromolecules* **1989**, *22*, 2396 and references therein.
(67) Connor, T. M.; Hartland, A. *Polymer* **1968**, *9*, 591.

MA950976+